15th World Congress on Computational Mechanics (WCCM-XV)
8th Asian Pacific Congress on Computational Mechanics (APCOM-VIII)
Virtual Congress: 31 July – 5 August 2022
S. Koshizuka (Ed.)

TIME-DEPENDENT MODELLING OF QUASI-BRITTLE MATERIALS WITH A STRONG DISCONTINUITY APPROACH

Saeed Mohammadzadeh Chianeh[1], **Daniel Dias-da-Costa**[1,*]

[1] School of Civil Engineering, The University of Sydney, Sydney, NSW 2006, Australia
[*] daniel.diasdacosta@sydney.edu.au

Key words: Time-dependent behaviour, Discrete Crack Approach, Finite Element Method, Coupled Algorithm

Abstract. *The time-dependent behaviour of quasi-brittle materials can have a significant effect on serviceability and ultimate failure. E.g., in the case of concrete structures, the presence of cracking can evolve, propagate and gradually widen over time, therefore significantly changing the stress state and expected structural response. The development of models that can account for the discrete nature of cracking whilst predicting time-dependent behaviour can be of interest to many practical applications. The discrete strong discontinuity approach (DSDA) has been validated as a reliable approach for simulating the cracking phenomenon by directly embedding the traction-separation constitutive relation within finite elements, therefore enriching standard finite element models with the ability to capture cracks, where material can separate without the need for remeshing. This work presents a generalisation to account for the long-term behaviour of cracked quasi-brittle materials, more specifically creep and shrinkage. To this end, a rate-type creep is first applied through a number of kelvin units; the interaction of the resulting response from the Kelvin chain system, shrinkage, and discrete cracking is developed to obtain a suitable constitutive model for the discrete crack simulations. Finally, the formulation is deployed on a finite element code where the performance of the proposed model is assessed through representative numerical examples.*

1 INTRODUCTION

A wide range of studies can be found in the literature related to the long-term behaviour of concrete structures [1-11]. Even though satisfactory results can often be obtained, there are many situations where a more accurate prediction of the time-dependent behaviour for cracked structures can require advanced models. In this domain, the discrete representation of cracks can better approximate discontinuous stress fields. With this in mind, this paper implements a finite element model for addressing the time-dependent behaviour of cracked concrete structures based on the DSDA [12].

2 Discrete strong discontinuity approach

The DSDA [12] can be formulated in the incremental form for a single element with an embedded strong discontinuity. Accordingly, at time step $n+1$:

$$\begin{bmatrix} \mathbf{K}^e_{aa} & -\mathbf{K}^e_{aw} \\ -\mathbf{K}^e_{wa} & \mathbf{K}^e_{ww}+\mathbf{K}^e_{d} \end{bmatrix}_{n+1} \begin{Bmatrix} \Delta\mathbf{a}^e_{n+1} \\ \Delta\mathbf{w}^e_{n+1} \end{Bmatrix} = \begin{Bmatrix} \Delta\mathbf{f}^e_{a_{n+1}} \\ \Delta\mathbf{f}^e_{w_{n+1}} \end{Bmatrix}, \quad (1)$$

where $\mathbf{a}^e$ is the vector of nodal displacements and $\mathbf{w}^e$ is the vector of nodal jumps at the discontinuity. The latter is measured at the two additional nodes i and j defined at both ends of the discontinuity – see Fig. 1 below. In this equation, the following definitions are applied:

$$\mathbf{K}_{aa}^{e,n+1} = \int_{\Omega\backslash\Gamma_d} \mathbf{B}^{e^T} D_{n+1}^{ve,e} \mathbf{B}^e d\Omega,\ \mathbf{K}_{aw}^{e,n+1} = \int_{\Omega\backslash\Gamma_d} \mathbf{B}^{e^T} D_{n+1}^{ve,e} \mathbf{B}_w^e d\Omega,\ \mathbf{K}_{wa}^{e,n+1} = \int_{\Omega\backslash\Gamma_d} \mathbf{B}_w^{e^T} D_{n+1}^{ve,e} \mathbf{B}^e d\Omega,$$
$$\mathbf{K}_{ww}^{e,n+1} = \int_{\Omega\backslash\Gamma_d} \mathbf{B}_w^{e^T} D_{n+1}^{ve,e} \mathbf{B}_w^e d\Omega,\ \mathbf{K}_d^e = \int_{\Gamma_d} \mathbf{N}_w^{e^T} T_w^e \mathbf{N}_w^e d\Gamma,$$
$$\Delta\mathbf{f}_{a_{n+1}}^e = \int_{\Omega\backslash\Gamma_d} \mathbf{N}^{e^T} \Delta\bar{\mathbf{b}}_{n+1}^e d\Omega + \int_{\Gamma_t} \mathbf{N}^{e^T} \Delta\bar{\mathbf{t}}_{n+1}^e\, d\Gamma + \int_{\Omega\backslash\Gamma_d} \mathbf{B}^{e^T} D_{n+1}^{ve,e} \Delta\varepsilon_{n+1}^{cs},\ \Delta\mathbf{f}_{w_{n+1}}^e = 0, \tag{2}$$

in which $\mathbf{B}_w^e = \mathbf{B}^e \mathbf{H}_{\Gamma_d}^e \mathbf{M}_w^{ek}$ and $\mathbf{N}_w^e$ is a matrix that contains the shape functions of the discontinuity and $\mathbf{M}_w^{ek}$ is composed of $\mathbf{M}_w(\mathbf{x})$ matrices evaluated at the element node coordinates and then stacked into rows:

$$\mathbf{M}_w(\mathbf{x}) = \begin{bmatrix} 1 - \frac{\left(x_2 - x_2^i\right)\sin\alpha}{l_d} & \frac{\left(x_2 - x_2^i\right)\cos\alpha}{l_d} & \frac{\left(x_2 - x_2^i\right)\sin\alpha}{l_d} & -\frac{\left(x_2 - x_2^i\right)\cos\alpha}{l_d} \\ \frac{\left(x_1 - x_1^i\right)\sin\alpha}{l_d} & 1 - \frac{\left(x_1 - x_1^i\right)\cos\alpha}{l_d} & -\frac{\left(x_1 - x_1^i\right)\sin\alpha}{l_d} & \frac{\left(x_1 - x_1^i\right)\cos\alpha}{l_d} \end{bmatrix}. \tag{3}$$

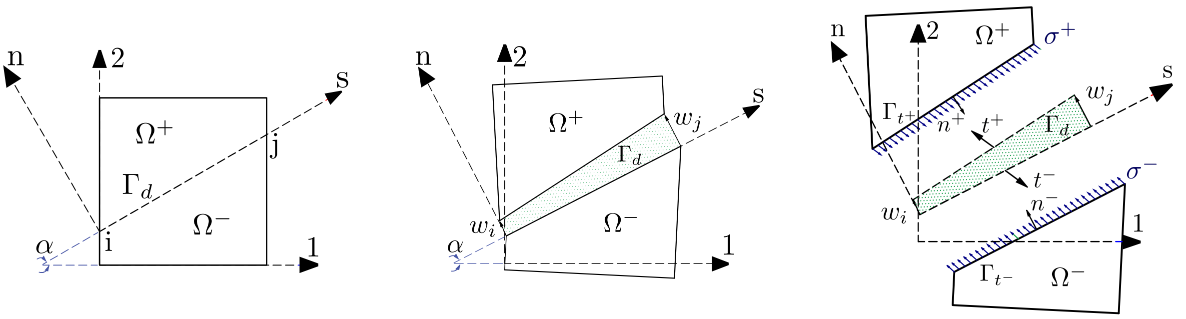

Figure 1: Strong discontinuity embedded on a bilinear element: (a) definitions; (b) crack opening; and (c) free Body diagram.

The DSDA separates the behaviour of the discrete embedded discontinuity from that of the bulk, and because of this the time-dependent behaviour can be easily incorporated into the formulation. This behaviour will be here approximated by a standard chain of components as represented in Fig. 2, where the bulk has the time-dependent components.

At the integration point level, the total strain can be written as:

$$\Delta\varepsilon_{n+1,j} = \Delta\tilde{\varepsilon}_{n+1,j} + \Delta\hat{\varepsilon}_{n+1,j} + \Delta\varepsilon_{n+1,j}^{cp} + \Delta\varepsilon_{n+1,j}^{sh}, \tag{4}$$

where $\Delta\tilde{\varepsilon}_{n+1,j}$, $\Delta\hat{\varepsilon}_{n+1,j}$, $\Delta\varepsilon_{n+1,j}^{cp}$, and $\Delta\varepsilon_{n+1,j}^{sh}$ are the increments of enhanced, bulk, creep, and shrinkage strains, respectively. Note that in the DSDA, the enhanced strain $\Delta\tilde{\varepsilon}_{n+1,j}$ in the cracked domain is zero. Thus, the stress-strain relation for integration point j at time step $n+1$ can be written as [13]:

$$\Delta\sigma_{n+1,j} = \mathbf{D}_{n+1,j}^{ve}(\Delta\varepsilon_{n+1,j} - \Delta\varepsilon_{n+1,j}^{cp} - \Delta\varepsilon_{n+1,j}^{sh}), \tag{5}$$

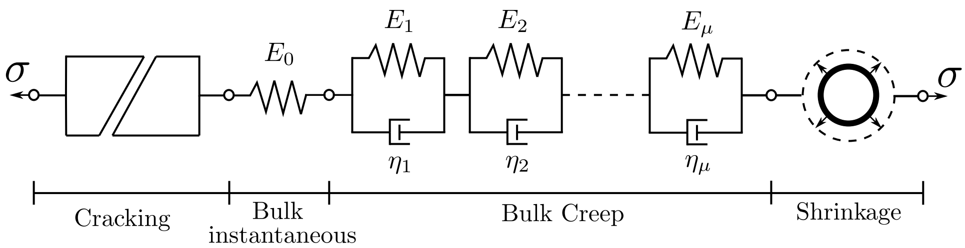

Figure 2: Constitutive behaviour of the different components.

where $\mathbf{D}_{ve}$ is the viscoelastic stress-strain relation matrix defined as:

$$\mathbf{D}^{ve}_{n+1,j} = E^{ve}_{n+1,j}\mathbf{G} \tag{6}$$

where $\mathbf{G}$ is the stress-strain relation matrix divided by the elastic modulus, E_0, and $E^{ve}_{n+1,j}$ is the viscoelastic modulus – see Fig. 2 – given by:

$$\frac{1}{E^{ve}_{n+1,j}} = \frac{1}{E_0} + \sum_{\mu=1}^{M} \frac{1}{E_{\mu_{n+1,j}}}, \tag{7}$$

where according to Fig. 2, E_0 is the modulus of elasticity of the bulk, and $E_{\mu_{n+1,j}}$ represents the spring stiffness (creep modulus) of the μ-th kelvin unit at the integration point j in the step $n+1$.

3 Incremental time-dependent strains

The modelling of the time-dependent behaviour based on rate-type creep or differential formulations can be computationally efficient. Additionally, a rate-type creep method can enable a more straightforward incorporation of the effects of other components, e.g. shrinkage, temperature, and the nonlinear effects of cracking and damage [14].

The increment of creep strain is split into viscous and viscoelastic increments, respectively corresponding to the unrecoverable and recoverable creep strain components, respectively:

$$\Delta\varepsilon^{cp}_{n+1,j} = \Delta\varepsilon^{f}_{n+1,j} + \Delta\varepsilon^{v}_{n+1,j}, \tag{8}$$

where the viscoelastic strain increment, $\Delta\varepsilon^{v}_{n+1,j}$, is calculated using the viscoelastic micro-strain creep increment, $\Delta\gamma_{i+1}$, as:

$$\Delta\varepsilon^{v}_{n+1,j} = \frac{\Delta\gamma_{n+1}}{\nu_{n+1/2}}, \tag{9}$$

where the micro-strain creep increment is obtained from solving the differential equation related to the μ-th kelvin unit using the first order exponential algorithm [14]:

$$\Delta\gamma_{\mu_{n+1}} = \gamma_{\mu_{n+1}} - \gamma_{\mu_n} = (1-\beta_{\mu_n})\left(\frac{\sigma_{n+1/2}}{E_\mu} - \gamma_{\mu_n}\right), \tag{10}$$

with β_{μ_n} being an auxiliary constant that simplifies the notation:

$$\beta_{\mu_n} = e^{-(\Delta t_n)/\tau_\mu}, \tag{11}$$

where, $\tau_\mu = \eta_\mu / E_\mu$ is called the retardation time, and $\nu_{n+1/2}$ in Eq. (9) is the volume of the solidified matter at the mid-time of a logarithmic time-step. This is calculated by:

$$\nu_{n+1/2} = \left[\sqrt{\frac{1}{t_{n+1/2}}} + \frac{q_3}{q_2} \right]^{-1}, \tag{12}$$

where $t_{n+1/2}$ denotes the mid-time of the logarithmic time-step:

$$t_{n+1/2} = t_0 + \left[(t_{n+1} - t_0)(t_n - t_0) \right]^{0.5}. \tag{13}$$

The increment of the viscous non-recoverable creep component is calculated by the following equation:

$$\Delta\varepsilon^{f}_{n+1,j} = \frac{G\sigma_{n-1/2} q_4 \Delta t_n}{t_{n+1/2}}, \tag{14}$$

where $\sigma_{n-1/2} = \sigma_{n-1} + \Delta\sigma/2$, and q_3 and q_4 are empirical material coefficients.

Shrinkage is treated as the drying component resulting from volume alterations in concrete as a result of evaporation [14]. Shrinkage is assumed direction independent and the shrinkage shear strain components are taken as zero. The shrinkage strain is here approximated by:

$$\varepsilon^{sh}_n = \frac{A t_n}{B + t_n}, \tag{15}$$

where A and B are determined from tests, and the shrinkage vector is obtained from $\varepsilon^{sh}_n \left[1\ 1\ 0 \right]^T$.

4 Case study

An experimental test is here presented to assess the performance of the formulation. The selected example is a four-point bending test carried under sustained loads for 380 days [15]. The geometry, reinforcement and the finite element model are represented in Fig. 3

The beam is modelled with 1,190 bilinear and 70 truss elements, respectively representing concrete and reinforcements. Only one-half of the beam was modelled to take advantage of the symmetry conditions of the problem – see Fig. 3(c). The characteristic concrete strength at 28 days was $f_{cm} = 24.8$ MPa and the modulus of elasticity was $E_c = 24950$ GPa. The concrete tensile strength was $f_{ct} = 2.8$ MPa at 28 days. The shrinkage constants from Eq. (15) were measured as $A_{sh} = 950\ \mu\varepsilon$ and $B_{sh} = 45$ days. The concrete fracture energy was taken as 75 N/m and the Poisson's ratio was assumed as $\nu = 0.2$. Perfect bond conditions were assumed between the reinforcement and concrete. The self-weight of concrete was taken as 23.5 kN/m^3 and the asymptotic elastic modulus of concrete for creep modelling was taken as $E_0 = 1.6E_{28} = 40GPa$. The empirical creep constants were measured by fitting the compliance data from a small creep test as: $q_2 = 186.5\ \mu\varepsilon$, $q_3 = 1.0\ \mu\varepsilon$/MPa, and $q_4 = 23.7\ \mu\varepsilon$/MPa. The retardation time and corresponding elastic moduli were taken as the same as in [15,16] (see Table 1). The calculated negative infinity area of the spectrum was $A_0 = 52.8$ MPa^{-1}.

Fig. 4 compares the results of time-dependent modelling with experimental data. As Fig. 4(a) shows the mid-span deflection where the proposed model compares relatively well with the experimental data.

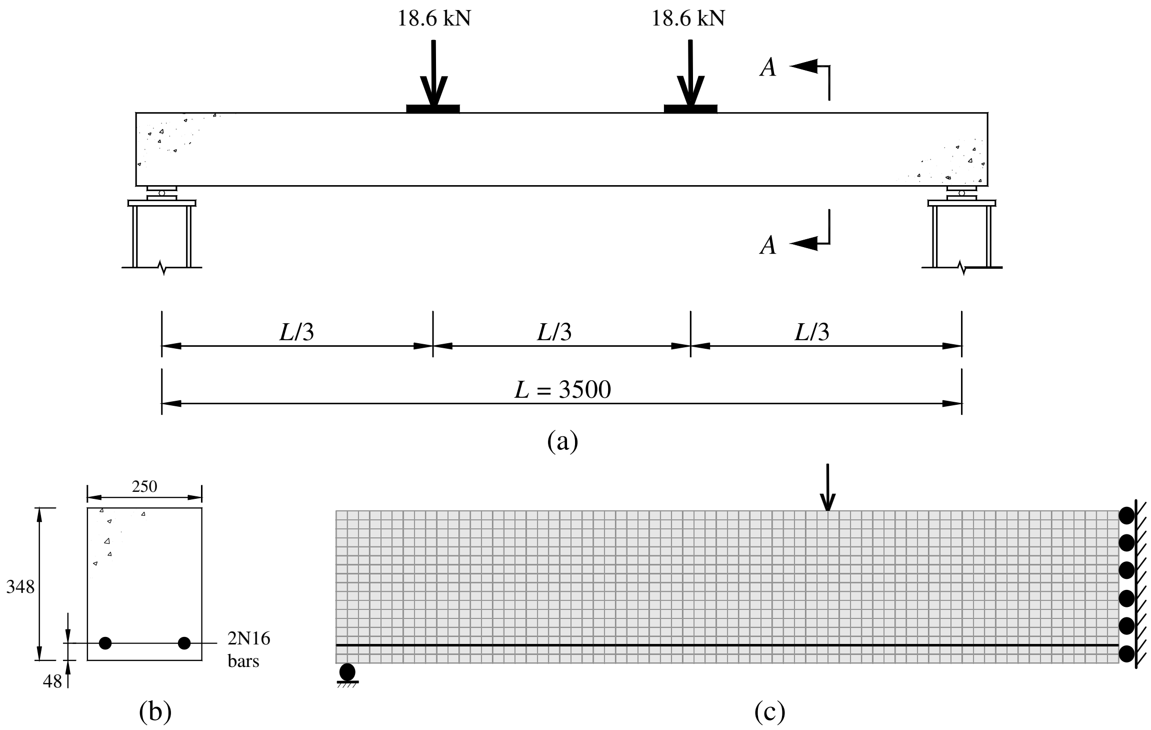

Figure 3: Four-point bending test: (a) overall geometry; (b) reinforcement details section A-A; (c) finite element model.

Table 1: Rheologic modelling data

μ	$\tau_\mu(days)$	E_μ
1	1e-4	0.08480
2	1e-3	0.07214
3	1e-2	0.06209
4	1e-1	0.05411
5	1e0	0.04778
6	1e1	0.04276
7	1e2	0.03877
8	1e3	0.03560

Regarding the maximum crack width shown in Fig. 4(b), some predicted points are closer to the experimental data than other models. Still, there are some differences that can be related to the perfect bond conditions assumed in the current implementation. At the last step of the analysis, the maximum experimental crack width is 0.381 mm, which compares against 0.402 mm and 0.355 mm, respectively, predicted by the DSDA and by [16]. Figs. 5(a) and (b) show the crack pattern and deflections of the beam at the beginning of the analysis and after creep has developed..

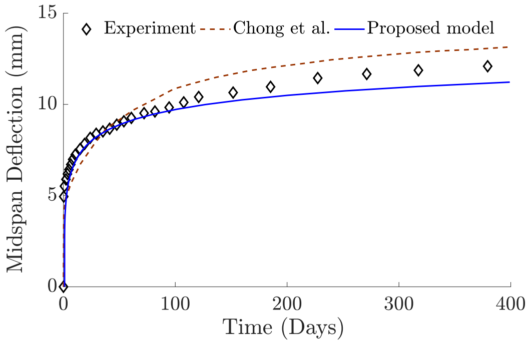

(a)

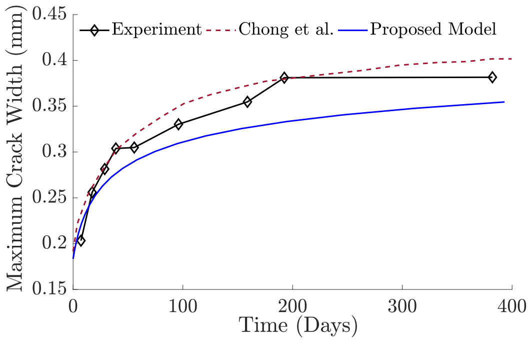

(b)

Figure 4: Four-point bending test: (a) Mid-span deflections vs. time; (b) Maximum crack width vs. time.

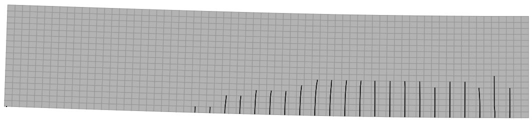

(a)

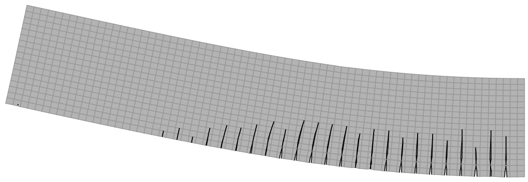

(b)

Figure 5: Four-point bending test (deflections amplified 20 times) (a) initial deflection (b) time-dependent deflection after 380 days.

5 CONCLUSIONS

A discrete model was implemented to address the time-dependent behaviour of reinforced concrete structures. The model was based on the DSDA, which was extended to include creep and shrinkage. The proposed model was validated against data available on a reinforced concrete beam under a four-point bending test. The results were compared with the ones obtained in another study using the smeared crack approach. In general, it was found that both models can provide reasonable estimates. However, it should be pointed out that a more detailed crack pattern could be presented with the discrete framework. Additionally, the discrete modelling offers significant potential for future studies based on the explicit implementations of other components, e.g. the bond-slip and rate-dependency of crack progression.

REFERENCES

[1] Tan, K.H. and Saha, M.K. Long-term deflections of reinforced concrete beams externally bonded with FRP system. *Journal of Composites for Construction* (2006) **10**(6):474–482.

[2] Bottoni, M. *Creep and damage models for the service behaviour of structural members*. alma, (2008)

[3] Tehami, M. and Ramdane, K.E. Creep behaviour modelling of a composite steel–concrete section. *Journal of Constructional Steel Research* (2009) **65**(5):1029–1033.

[4] Hamed, E. and Bradford, M.A. Creep in concrete beams strengthened with composite materials. *European Journal of Mechanics-A/Solids* (2010) **29**(6):951–965.

[5] Hamed, E. and Bradford, M.A. Flexural time-dependent cracking and post-cracking behaviour of FRP strengthened concrete beams. *International Journal of Solids and Structures* (2012) **49**(13):1595–1607.

[6] Hamed, E. and Chang, Z.T. Effect of creep on the edge debonding failure of FRP strengthened RC beams–A theoretical and experimental study. *Composites science and technology* (2013) **74**:186–193.

[7] Garcia-Taengua, E. and Arango, S. and Marti-Vargas, J.R. and Serna, P. Flexural creep of steel fiber reinforced concrete in the cracked state. *Construction and Building Materials* (2014) **65**:321–329.

[8] Hazelwood, T. and Jefferson, A.D. and Lark, R.J. and Gardner, D.R. Numerical simulation of the long-term behaviour of a self-healing concrete beam vs standard reinforced concrete. *Engineering Structures* (2015) **102**:176–188.

[9] Nguyen, Q.H. and Hjiaj, M. Nonlinear Time-dependent behavior of composite steel-concrete beams. *Journal of Structural Engineering* (2016) **142**(5):04015175.

[10] Hadjazi, K. and Sereir, Z. and Amziane, S. Creep response of intermediate flexural cracking behavior of reinforced concrete beam strengthened with an externally bonded FRP plate. *International Journal of Solids and Structures* (2016) **102**:196–205.

[11] Boumakis, I. and Di Luzio, G. and Marcon, M. and Vorel, J. and Wan-Wendner, R. Discrete element framework for modeling tertiary creep of concrete in tension and compression. *Engineering Fracture Mechanics* (2018) **200**:263–282.

[12] Dias-da-Costa, D. and Alfaiate, J. and Sluys, L.J. and Julio, ENBS. A discrete strong discontinuity approach. *Engineering Fracture Mechanics* (2009) **76**(9):1176–1201.

[13] Bazant, Z. P. *Mathematical modeling of creep and shrinkage of concrete*. Wiley, (1988)

[14] Bažant, Z.P. and Jirásek, M. *Creep and hygrothermal effects in concrete structures*. Springer. (2018) **38**:263–282.

[15] Gilbert, R.I. and Nejadi, S. *An experimental study of flexural cracking in reinforced concrete members under sustained loads*. University of New South Wales, School of Civil and Environmental Engineering. (2004)

[16] Chong, K.T. and Foster, S.J. and Gilbert, R.I. Time-dependent modelling of RC structures using the cracked membrane model and solidification theory. *Computers & structures* (2008) **86**(11-12):1305–1317.